Coordination Chemistry Reviews 255 (2011) 2594–2601

Contents lists available at ScienceDirect

Coordination Chemistry Reviews

journal homepage: www.elsevier.com/locate/ccr

Review

Photoinduced water oxidation using dendrimeric Ru(II) complexes as photosensitizers

Fausto Puntoriero[a], Andrea Sartorel[b], Michele Orlandi[c], Giuseppina La Ganga[a], Scolastica Serroni[a], Marcella Bonchio[b,*], Franco Scandola[c,*], Sebastiano Campagna[a,*]

[a] Dipartimento di Chimica Inorganica, Chimica Analitica e Chimica Fisica, Università di Messina and Centro Interuniversitario per la Conversione Chimica dell'Energia Solare, sezione di Messina, Via Sperone 31, 98166 Messina, Italy
[b] ITM-CNR and Department of Chemical Sciences, University of Padova, Via Marzolo, 1, 35131 Padova, Italy
[c] Dipartimento di Chimica and Centro Interuniversitario per la Conversione Chimica dell'Energia Solare, sezione di Ferrara, Via Borsari 49, 49100 Ferrara, Italy

Contents

ARTICLE INFO

Article history:
Received 14 October 2010
Accepted 18 January 2011
Available online 26 January 2011

Keywords:
Artificial photosynthesis
Photoinduced water splitting
Water oxidation
Electron transfer
Metal dendrimers

ABSTRACT

Following bio-inspired guidelines, solar-powered water oxidation can be exploited for hydrogen generation by direct photocatalytic water splitting. This reaction poses some formidable challenges at the interface of oxidation catalysis and photochemistry. Molecular innovation is expected to provide a decisive lead in the field of artificial photosynthesis. Key achievements include the discovery of novel transition metal catalysts, exhibiting oxygen-evolving activity upon multi-electron oxidation and the design of antenna-like sensitizers. The thermodynamic and photophysical requirements of the system are discussed herein. A successful combination is obtained with polynuclear dendrimeric Ru(II) polypyridine sensitizers, activating colloidal IrO_2 nanoparticles or a tetra-ruthenate polyoxometalate catalyst. In this latter case, an unprecedented quantum yield up to 30% is achieved, which holds great promise for the up-grade to functional materials and practical technology.

1. Introduction

Artificial photosynthesis is a Holy Grail of modern science [1–7]. Actually, the effective production of high-energy content chemical species, i.e. fuels, by exclusively using solar irradiation would revolutionize modern society, giving access to a virtually inexhaustible energy source, equally distributed on Earth. Search on artificial photosynthesis has therefore been extremely appealing in the last decades, and has become more and more urgent as the global energy demand is deemed to increase substantially in the very next future.

To develop synthetic systems capable of performing artificial photosynthesis, Nature is obviously the ideal model; analogous to the natural photosynthetic systems, a synthetic system capable of performing artificial photosynthesis should contain the following basic components: (i) light-harvesting antennae; (ii) charge separation units; (iii) multielectron transfer catalysts (see Fig. 1) [8,9]. Whereas the design of light-harvesting antenna systems as well as of charge separation units have been extensively pursued in the last decades, with quite remarkable results [5–13], the bottleneck of research in artificial photosynthesis has been the design of

* Corresponding authors. Tel.: +39 090 6765737; fax: +39 090 393756.
E-mail addresses: marcella.bonchio@unipd.it (M. Bonchio), snf@unife.it (F. Scandola), campagna@unime.it (S. Campagna).

0010-8545/$ – see front matter © 2011 Elsevier B.V. All rights reserved.
doi:10.1016/j.ccr.2011.01.026

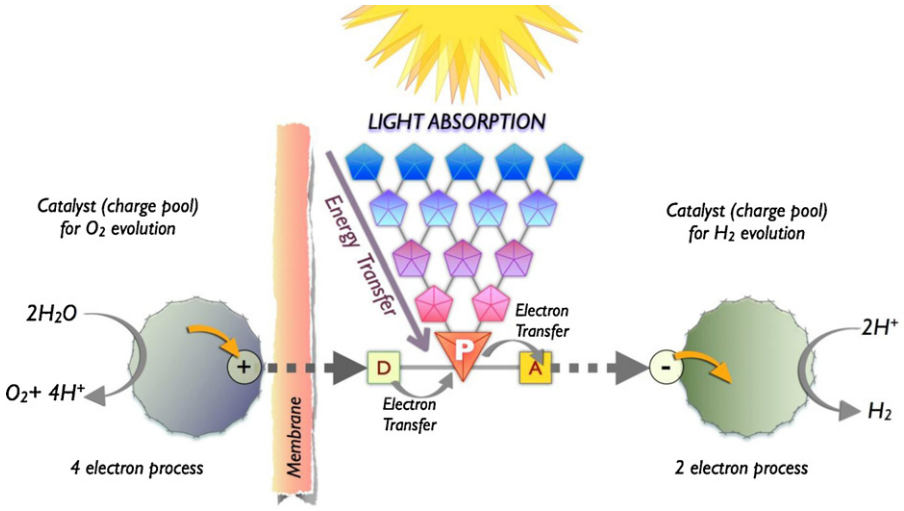

Fig. 1. Schematic representation of an artificial photosynthetic system.

synthetic catalysts capable of driving light-induced multielectron transfer processes, efficiently. In particular, as any scheme of artificial photosynthesis must include water oxidation, photo-driven production of molecular oxygen from water is the fundamental step that has to be pursued towards the achievement of an efficient artificial photosynthesis [14–17].

Water oxidation to molecular oxygen is indeed a quite complex reaction: it requires a four electron exchange, and orchestrating bond breaking-forming events as a new O–O bond should be the final outcome. Eq. (1) indicates that such a reaction requires a potential E (vs NHE) of 1.23 eV (at pH 0), whereas the global process highlighted in Eq. (2) is endoergonic by 4.92 eV (113.38 kcal).

$$2H_2O \rightarrow O_2 + 4e^- + 4H^+ \quad (E = +1.23 - 0.059 \times \mathrm{pH})\,\mathrm{V} \qquad (1)$$

$$2H_2O \rightarrow O_2 + 2H_2 \quad (\Delta G = +4.92\,\mathrm{eV}) \qquad (2)$$

In green plants and some bacteria, the quite complex reaction shown in Eq. (1) is performed by part of Photosystem II, known as the oxygen evolving complex (OEC), whose structure was finally clarified a few years ago [18]: this OEC is made of a cluster of four manganese and one calcium ion, held together by oxygen bridges. The five redox states which are sequentially involved in the overall four-electron process needed to perform water oxidation (the so-called Kok cycle [19]) are related to proton-coupled electron transfer steps [14,15,20]. The OEC is one of the more oxidizing natural systems. Even Nature finds water oxidation a quite difficult task: under ambient sunlight in the chloroplast, the OEC must be re-synthesized every half an hour owing to the oxidation damage it undergoes from the oxygen that itself has produced [17].

A synthetic, non-protein catalyst capable of oxidizing water as effectively as the OEC was prepared about 30 years ago [21]. This was the so-called "blue dimer", whose structural formula is shown in Fig. 2 (the "blue dimer" is compound b; in this figure other molecular catalysts, successively made, are shown). Once activated electrochemically or chemically, via a strong oxidizing agent (e.g., cerium salts), the blue dimer undergoes the stepwise loss of four electrons and four protons, producing an intermediate species that oxidizes water [21,22]. Unfortunately, the blue dimer loses its catalytic efficiency after a few cycles. However, the blue dimer paved the way to the discovery of other water oxidation catalysts, most of them still based on ruthenium centers [23–26]. In the last few years, also molecular catalysts based on iridium centers [27], as well as on cheaper metals such as manganese [28,29], cobalt [30], and iron [31] have been prepared. Interestingly, whereas most of the molecular catalysts reported are, inspired by the natural OEC, multimetallic species, some recent reports have suggested that also monometallic systems can behave as effective catalysts [27,31–33]. Among such monometallic species, even osmium compounds have been introduced [34].

Beside the molecular catalysts mentioned above, colloidal systems have also been employed as catalysts for water oxidation:

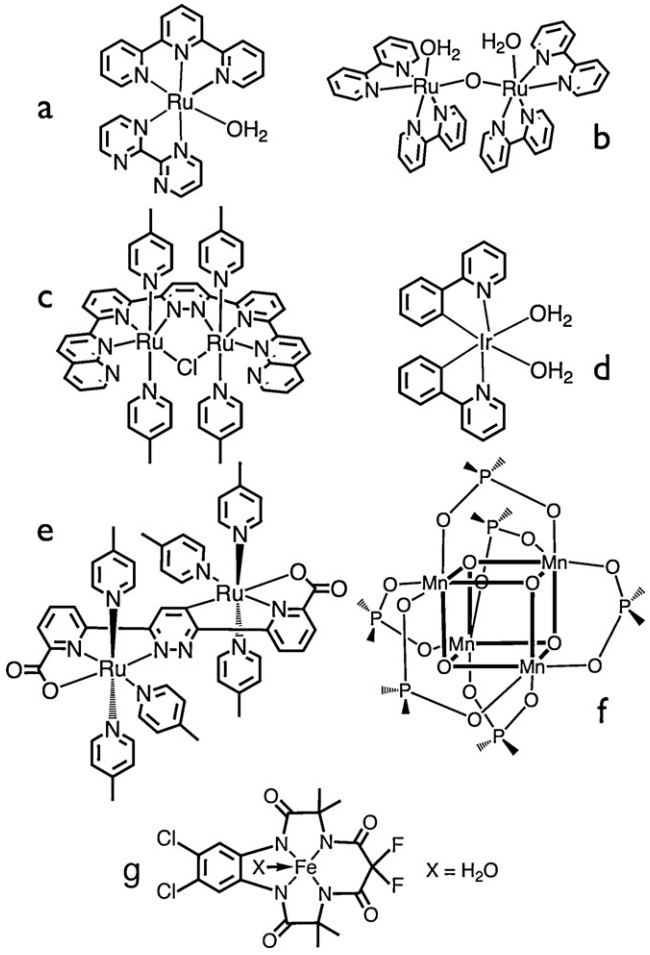

Fig. 2. Some examples of molecular catalysts for water oxidation. The "blue dimer" is compound b. Charges of the ionic species are omitted. For details, see Refs. [32] (for compound a); [21] (b); [33] (c); [27] (d); [24b] (e); [29] (f); [31] (g).

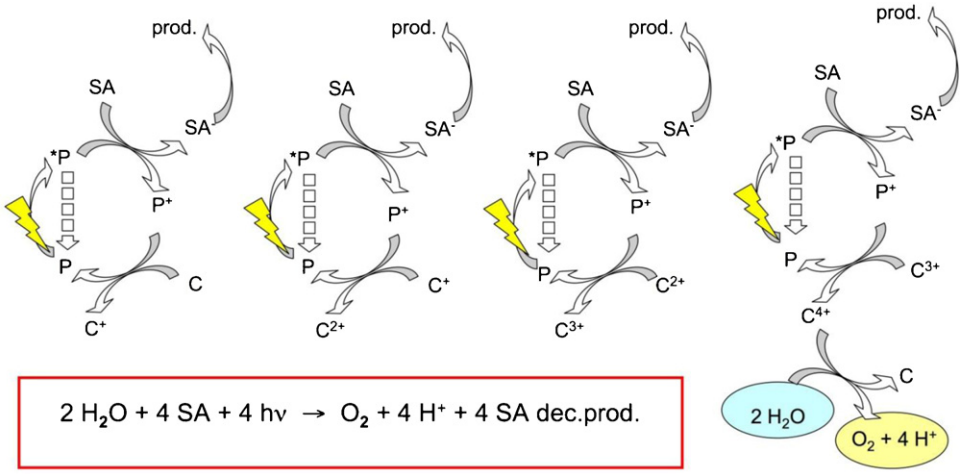

Fig. 3. Schematization of the main reactions involved in the photoinduced water oxidation processes.

within this class, prominent roles have been played by metal oxides [35,36], including iridium oxide nanoparticles introduced in the eighties [37] and more recently optimized [38–40].

Very interesting and promising results have been recently obtained by using cobalt and phosphate salts to spontaneously arrange, under specific conditions, an efficient catalyst system which features, beside self-assembly, self-healing properties, both typical properties of the natural systems [41–44].

Most of the catalysts mentioned above have been investigated by electrochemical or chemical activation, analogously to the blue dimer behavior. Only a few of them take advantage of photo-activation [36,45–50]. In this regard, the most common photosensitizer used is $[Ru(bpy)_3]^{2+}$ (bpy = 2,2′-bipyridine), although porphyrins have also been employed [51]. The choice of $[Ru(bpy)_3]^{2+}$ as the photosensitizer is due to the quite interesting and convenient properties of such a species, including absorption in the visible region, relatively long-lived excited-state lifetime, reversible redox processes, and stability in the ground and excited states [52,53]. However, $[Ru(bpy)_3]^{2+}$ has only limited absorption in the visible, so for taking full advantage of solar radiation, sensitizers having a larger cross section with solar light are desired. In the last 20 years, some of us have been involved in the design and study of the photophysical and redox properties of multinuclear Ru(II) and Os(II) dendrimers [54–60]. These compounds seem to be ideal photosensitizers for photoinduced water oxidation, for several reasons. Here we will focus on the results we have obtained in the very recent few years on photoinduced water oxidation by using multinuclear Ru(II) dendrimers as photosensitizer.

2. Photoinduced water oxidation. A general scheme

Eqs. (3)–(13) illustrate a possible general scheme for photoinduced water oxidation assisted by a sacrificial acceptor. In such equations, P, SA, and C are the photosensitizer, the (primary acceptor) sacrificial agent, and the catalyst, respectively. Once formed by sunlight (Eq. (3)), *P undergoes oxidative electron transfer in the presence of a primary acceptor, the sacrificial agent SA, leading to the formation of the oxidized photosensitizer, P^+ (Eq. (4)). Eq. (5), decay of P* to the ground state P, is a competing reaction, and the ratio between Eqs. (4) and (5) rate constants determines the efficiency of P^+ production, which can be optimized (i.e., made equivalent to 1) by adjusting the concentration of SA. Eq. (6), back electron transfer between P^+ and SA^-, is a poisoning reaction for the overall process, however it can be eliminated if the sacrificial agent rapidly decomposes upon reduction, as it is the case of the persulfate anion.

$$P + h\nu \rightarrow {}^*P \quad (3)$$

$${}^*P + SA \rightarrow P^+ + SA^- \quad (4)$$

$${}^*P \rightarrow P + h\nu' \text{and/orheat} \quad (5)$$

$$P^+ + SA^- \rightarrow P + SA \quad (6)$$

$$SA^- \rightarrow \text{products} \quad (7)$$

$$P^+ + C \rightarrow P + C^+ \quad (8)$$

Once formed, P^+ reacts with C, leading to the restoration of the ground state photosensitizer P, which is ready for another cycle, and to the formation of the mono-oxidized catalyst (Eq. (8)).

$$P^+ + C^+ \rightarrow P + C^{2+} \quad (9)$$

$$P^+ + C^{2+} \rightarrow P + C^{3+} \quad (10)$$

$$P^+ + C^{3+} \rightarrow P + C^{4+} \quad (11)$$

$$P* + C^{n+} \rightarrow P^+ + C^{(n-1)+} \quad (12)$$

$$C^{4+} + 2H_2O \rightarrow C + O_2 + 4H^+ \quad (13)$$

Eqs. (9)–(11) are the successive, stepwise oxidations of C^+ by P^+ ultimately leading to C^{4+}, the needed active catalyst that can oxidize water (Eq. (13)). Thermodynamics factors are expected to be different for the various stepwise mono-oxidation processes showed in Eqs. (8)–(11). Eq. (12) is another poisoning reaction, which can involve any C^{n+} species (with $n = 1$–3) and could compete with Eq. (4); Eq. (12) can be minimized by keeping low the concentration of C. Please note that in the above scheme, it is implicitly assumed that SA is a chemical species; also a semiconductor electrode can take this role (see Ref. [61] for an example): in this latter case, the optimization of Eq. (4) vs Eq. (5) reactions can be obtained by modifying the level of the semiconductor conduction band by an applied bias, and the irreversibility in the overall process is given, rather than by Eq. (7), by removal of the negative charge from SA^- via an external circuit. The main reactions involved in the overall photoinduced water oxidation process are illustrated in Fig. 3.

Since four photoinduced cycles are needed to produce the active C^{4+} catalyst form, the photochemical quantum yield of molecular oxygen produced, $\Phi(O_2)$, calculated by Eq. (14), can reach a limiting value of 0.25, unless some radical process is involved. Actually, in the specific (but quite common) case when persulfate ions are used as the sacrificial agent SA, the limiting value can reach 0.5, as the product of the reaction in Eq. (4) is the sulfate radical anion, which can promptly react with P to generate another molecule of oxidized

photosensitizer P^+ or could directly react with $C^{(n-1)+}$ to form C^{n+}. In both cases, two photons are needed for producing a molecule of oxygen.

$$\Phi(O_2) = \frac{(\text{moles of } O_2 \text{ produced})}{(\text{moles of absorbed photons})} \quad (14)$$

3. Some requirements for the photosensitizer for water oxidation. The convenience of Ru(II) polypyridine complexes

Looking at Eqs. (3)–(13), the first requirement is that (i) P absorbs as much visible light as possible. Then (ii) it has to undergo a fast and efficient photoinduced electron transfer leading to P^+, so that the ratio between rate constants of Eqs. (4) and (5) approaches 1. To this aim, a long-lived excited state of P^* is highly desired, as this means that Eq. (5) is not extremely fast, and it is also required that the reducing power of P^* is enough to make Eq. (4) feasible from a thermodynamic viewpoint. Moreover, (iii) the oxidized sensitizer P^+ must have a suitable potential to allow the reactions in Eqs. (8)–(11) to occur. In other word, the oxidation potential of the redox couple P^+/P (E_{ox} (P^+/P)) must be more positive than that of the redox couple C^{4+}/C^{3+} (which of course is the more positive potential of any $C^{n+}/C^{(n-1)+}$ couples involved in Eqs. (8)–(11)), so that all the mono-electronic stepwise electron transfer processes leading to C^{4+} shown in Eqs. (8)–(11) are thermodynamically favored. In general, from the above discussion it is clear that the oxidation potential of the redox couple P^+/P must be as much positive as possible. In any case, as the redox potential needed to oxidize water is 1.23 V vs NHE, so that the potential of the couple C^{4+}/C^{3+} at least has to be more positive than this value, 1.23 V vs NHE is the low limit for the potential of the P^+/P couple, although obvious kinetic reasons suggest that the effective potential of the P^+/P couple should be substantially more positive than this limit to allow for efficient processes to occur (it should be recalled, however, that the +1.23 V vs NHE value is pH-dependent, see Eq. (1)).

The above mentioned requirements (i)–(iii) clarify why Ru(II) polypyridine complexes, in particular the prototype $[Ru(bpy)_3]^{2+}$, have been extensively used as photosensitizers. Actually, the excited state of $[Ru(bpy)_3]^{2+}$ is a triplet metal-to-ligand charge-transfer (^{3}MLCT) state, having an excited-state energy of about 2.12 eV with a lifetime close to 0.5 μs and a luminescence quantum yield of 0.028, in air-equilibrated aqueous solution [52,62]. Such excited-state properties indicate that the decay processes leading to the ground state in $[Ru(bpy)_3]^{2+}$ are relatively slow. In fact, the ^{3}MLCT state of $[Ru(bpy)_3]^{2+}$ can be involved in many efficient electron transfer processes, also owing to the mild and reversible redox properties of the compound. Noticeably, the oxidation potential of $[Ru(bpy)_3]^{2+}$ in aqueous solution is +1.26 V vs SCE, that is ca. +1.51 V vs NHE, fulfilling the requirement (iii) discussed above. However, multinuclear Ru(II) dendrimers based on 2,3-bis(2′-pyridyl)pyrazine (dpp) bridging ligands offer several advantage over $[Ru(bpy)_3]^{2+}$-type compounds as photosensitizers in water oxidation, in particular as far as requirements (i) and (iii) are concerned.

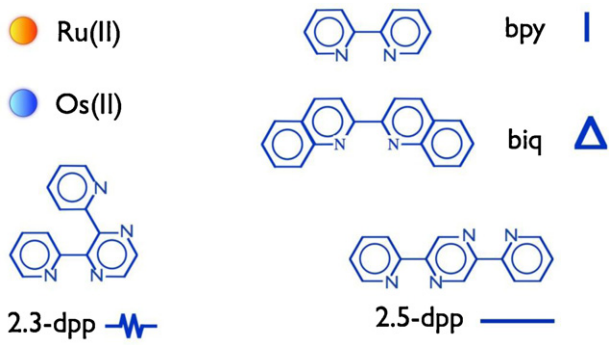

Fig. 4. Some components (and their representations) used for the synthesis of Ru(II) dendrimers. For details, see Refs. [54–56].

4. Multinuclear Ru(II) dendrimers based on dpp bridging ligands and their advantages over monomeric $[Ru(bpy)_3]^{2+}$-type compounds for photoinduced water oxidation

Ru(II) and Os(II) dendrimers based on dpp bridging ligands have been extensively investigated by some of us during the last 20 years [54–60]. Dozens of compounds have been synthesized and studied. Fig. 4 shows some components used, which also includes the isomeric 2,5-bis(2′-pyridyl)pyrazine bridge (2,5-dpp) as bridging ligands, and 2,2′-biquinoline (biq) as peripheral ligands [56]. Fig. 5 shows a schematization of the first, second, and

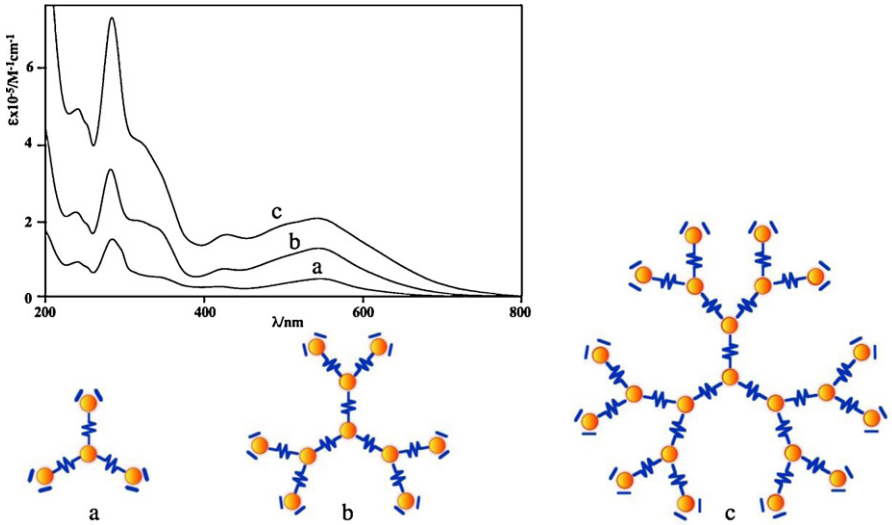

Fig. 5. Schematization of Ru(II) dendrimers containing four (a), ten (b), and twenty-two (c) metal centers. Compounds (a), (b), and (c) are called **4**, **10**, and **22**, respectively, in the main text. The inset shows the relative absorption spectra in acetonitrile [54].

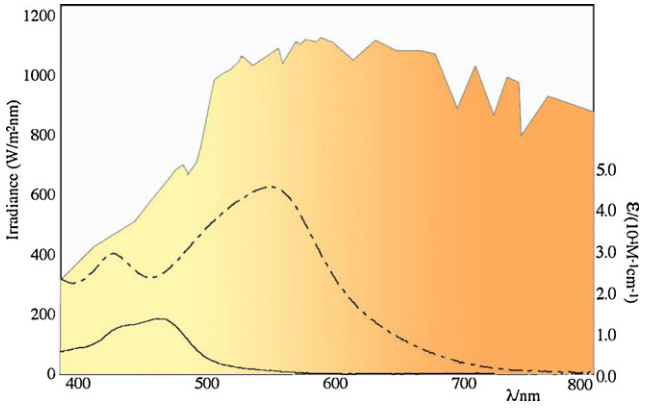

Fig. 6. Absorption spectra of $[Ru(bpy)_3]^{2+}$ (solid line) and **4** (dotted-dashed line) in aqueous solution and their comparison with the solar spectrum at the sea level [63].

third generation dendrimers – containing, four, ten, and twenty two metal centers, respectively – based on Ru(II) metal centers, bpy as peripheral ligands and dpp as bridging ligands. For this series of compounds, the absorption spectrum extends beyond 700 nm, due to MLCT bands involving both peripheral bpy and bridging dpp ligands as acceptors. The intense lowest energy MLCT absorption bands, responsible for the low energy band maximizing at about 545 nm, is due to spin-allowed MLCT transitions involving the peripheral metal center(s) as donor and the bridging ligand(s) as the acceptor. The absorption spectra of such compounds are essentially additive, so that on passing from compound **4** to **10** and **22** (compounds a, b, and c, respectively, in Fig. 5) their molar absorption increases accordingly to the number of chromophores, still keeping the shape constant (see Fig. 5, inset). For all the compounds shown in Fig. 5, the lowest-lying ^{3}MLCT state, populated with unitary efficiency from any upper lying excited state, takes place in the subpicosecond timescale. In other words, ultrafast energy transfer occurs from the higher energy MLCT states involving inner Ru(II) centers to the lower-lying MLCT states, involving peripheral metal centers [54–60]. The lower-lying excited state, identical in nature for all the series of compounds, emits at about 780 nm in aqueous solution at room temperature, with a lifetime of 30 ns (60 ns in acetonitrile solution) and a quantum yield of 0.002 (0.003 in acetonitrile). The emission spectrum is shifted to the blue, maximizing at 725 nm, in rigid matrix at 77 K. Interestingly, the first oxidation potential of **4**, **10** and **22** occurs around 1.55 V vs SCE in acetonitrile solution (+1.45 V in aqueous solution, that is +1.70 V vs NHE) and involves the practically simultaneous one-electron oxidation of all the equivalent peripheral metal centers.

As far as the above mentioned requirements (i), the cross section with solar spectrum, and (iii) the potential of the P^+/P couple, are concerned, clearly compounds like the tetranuclear **4** species have much better properties than the mononuclear $[Ru(bpy)_3]^{2+}$. Fig. 6 shows the different overlap of **4** and $[Ru(bpy)_3]^{2+}$ with the solar spectrum at the sea level: beside the higher molar absorbance at all wavelengths, **4** covers much better the red portion of solar spectrum; from the oxidation potential values, about 200 mV of difference make the oxidized form of **4** more effective than the oxidized form of $[Ru(bpy)_3]^{2+}$ to extract electrons from the various redox state of the catalyst C. This means that all the reactions in Eqs. (8)–(11) are about 200 mV more favorable when **4** replaces $[Ru(bpy)_3]^{2+}$ as the oxidized photosensitizer. However, it has also been mentioned a somewhat negative point: the excited state of **4** is less reducing that that of $[Ru(bpy)_3]^{2+}$: in fact the oxidation potential of the MLCT state of **4** is only +0.2 V vs SCE, requiring a very good SA to allow Eq. (4) to be efficient.

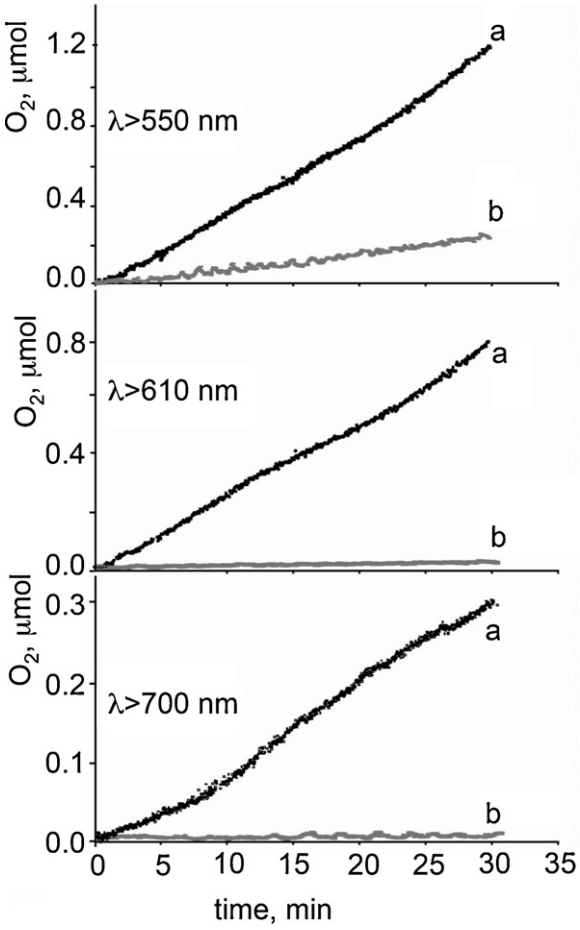

Fig. 7. Time profile of oxygen evolution during continuous irradiation of solutions containing **4** (curves a) or $[Ru(bpy)_3]^{2+}$ (curves b) as the sensitizer, citrate-stabilized IrO_2 nanoparticles, and persulfate. Irradiation wavelengths are shown in the figure. For details, see Ref. [63].

5. The tetranuclear Ru(II) dendrimer and photoinduced water oxidation

5.1. The tetranuclear dendrimer and colloidal oxygen-evolving catalysts

The first use of a Ru(II) dendrimer as a photosensitizer for photoinduced water oxidation was made by coupling compound **4**, the simplest dendrimer of the series, with IrO_2 nanoparticles as the water oxidation catalyst [63]. Colloidal IrO_2 was introduced as a water oxidation catalyst more than 20 years ago [37], however only recently has its use been optimized by preparing nanoparticles [38–40]. Quite recently, also a functional photoelectrochemical cell for photoassisted overall water splitting has been made [61]. In all these studies, the photosensitizer was a Ru(II) polypyridine monomer. To compare the performance of Ru(II) dendrimeric systems in comparison with the usually used Ru(II) monomer species as photosensitizers in water oxidation processes, we performed photoinduced water oxidation by using citrate-stabilized IrO_2 nanoparticles as OEC in the presence of persulfate anions as the sacrificial agent in aqueous buffered solution and taking advantage of $[Ru(bpy)_3]^{2+}$ or **4** as sensitizers. Different wavelengths were used to produce the sensitizer excited state. The result of the comparison is shown in Fig. 7. Indeed, as expected on the basis of the absorption spectra of $[Ru(bpy)_3]^{2+}$ and **4**, the efficiency of oxygen production was much larger by using equimolar solution of **4** vs $[Ru(bpy)_3]^{2+}$ upon irradiating the reaction solution with light having $\lambda > 500$ nm.

Even more interesting, the system containing **4** as sensitizer is still active when light with $\lambda > 700$ nm is used, a condition in which the system containing **1** is obviously not active since this latter compound does not absorb in this condition. The efficiency of oxygen production at the various excitation wavelengths is proportional to the molar absorption of **4** in the visible region, so indicating that quantum yield of oxygen production is constant regardless excitation wavelength, and therefore that the light energy absorbed by any component of the tetranuclear (supramolecular) species equally contributes to oxygen production. In other words, the system based on **4**/IrO_2/persulfate incorporates a light-harvesting antenna (the tetranuclear sensitizer), a charge separation device (made by the combination of SA, P, and C) and the OEC. The photochemical quantum yield for oxygen production, calculated at the fixed excitation wavelength of 550 nm, was 0.015 [63], a figure that anyway could be easily increased, considering that the IrO_2 nanoparticles used were not optimized. Actually, in successive experiments using optimized (malonate-stabilized) nanoparticles a quantum yield of 0.055 was obtained [64].

The major drawback of IrO_2 nanoparticles as OEC seems to be a relatively slow electron transfer between the oxidized sensitizer and IrO_2, that is the reaction in Eq. (8) (and probably the same problem is also present for the reactions leading to accumulation of the needed four holes in the IrO_2 nanoparticles, Eqs. (9)–(11)). This slow electron transfer, measured by Mallouk and coworkers in homogeneous solution [38] and occurring in the ms timescale regime, is held responsible for the relatively low efficiency of the photo-assisted electrochemical cell based on Ru(II) polypyridine monomer as sensitizer to which IrO_2 nanoparticles are tethered via carboxylate substituent and using TiO_2 nanoparticles as anode [61]. In fact, a photochemical quantum yield value of 0.0018 is found for oxygen production in such a photoelectrochemical cell. The slow electron transfer between P^+ and the carboxylate-connected IrO_2 in fact makes this latter process weakly competitive with charge recombination from the "reduced" TiO_2 electrode and P^+ (in the scheme in Section 2, this corresponds to the poisoning reaction schematized in Eq. (6)). Moreover, even when SA which rapidly decomposes upon reduction (as persulfate anions) is used, so minimizing Eq. (6), the slow electron transfer between P^+ and IrO_2 nanoparticles (actually, a hole scavenging process) can lead to photosensitizer decomposition, as P^+ can be attacked by the O_2 produced, so finally leading to deactivation of the catalytic process. This is actually the reason suggested for the decomposition of Ru(II) polypyridine complexes during the water oxidation catalyzed by IrO_2 catalysts [65]. The hole scavenging processes discussed above (i.e., the series of reactions shown in Eqs. (8)–(11)) should be more efficient on replacing $[Ru(bpy)_3]^{2+}$ with **4**, because of the about 200 mV of favorable difference in the potential of the P^+/P redox couple in case of **4**, as mentioned above. As a consequence, the system using **4** as the sensitizer instead of $[Ru(bpy)_3]^{2+}$ should be more stable. However, a faster hole scavenging process was definitely desired.

5.2. The tetranuclear dendrimer and a molecular catalyst. Fast hole scavenging and the 4 × 4 ruthenium interplay

A quite interesting and efficient molecular oxygen evolving catalyst was introduced a couple of years ago. It is a fully inorganic compound made of a four ruthenium(IV) core, with oxygen and hydroxo bridges, stabilized by two polyoxometalated caps, whose formula is $[Ru_4(\mu\text{-}O)_4(\mu\text{-}OH)_2(H_2O)_4(\gamma\text{-}SiW_{10}O_{36})_2]^{10-}$ (see Fig. 8; herein after, this species is called **Ru4(POM)**) [25,26,66–68]. The all-inorganic nature of the catalyst would explain, according to the authors, the stability of the compound during the catalytic process, different from the other molecular catalysts shown in Fig. 2, whose instability has been attributed

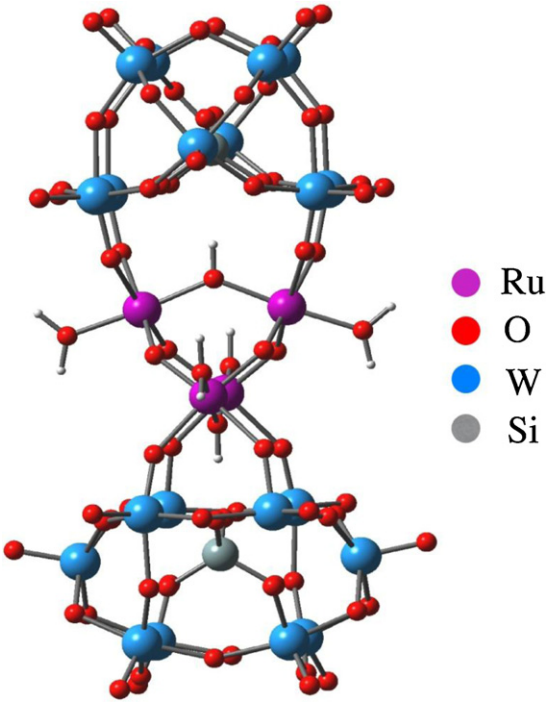

Fig. 8. Structure of the oxygen evolving catalyst made of a four-ruthenium core and two polyoxometalate caps [25,26].

to attack of the oxygen produced on the organic ligands. Indeed, the **Ru4(POM)** catalyst is very stable and efficient, with turnover frequencies up to 0.60 s^{-1} obtained for electrochemically or chemically driven water oxidation processes, which compares well with other top-performing molecular catalysts [69]. These latter, however display an intrinsic structural weakness due to the labile coordination sphere, and fast turnover regime is generally observed only for a limited period, thus precluding long-term applications.

A fast electron transfer process between the chemical oxidant and the catalyst could contribute to the high turnover frequency of **Ru4(POM)** in chemically driven water oxidation processes. This electron transfer has been kinetically investigated by using $[Ru(bpy)_3]^{3+}$, photochemically generated by $[Ru(bpy)_3]^{2+}$ in the presence of persulfate anions [70]. In a typical nanosecond laser flash photolysis experiment (excitation, 355 nm; FWHM, 8 ns), the recovery of the bleach at 450 nm, due to the regeneration of $[Ru(bpy)_3]^{2+}$, is accelerated on increasing **Ru4(POM)** concentration (see Fig. 9). The kinetics (pseudo-first order, $[\mathbf{Ru4(POM)}] \gg [[Ru(bpy)_3]^{3+}]$), which depend on catalyst concentration, lead to an average bimolecular rate constant of $(2.1 \pm 0.4) \times 10^9\ M^{-1}\ s^{-1}$ for the process (the hole scavenging shown in Eq. (8)), close to the diffusion-controlled limiting rate. Clearly, from a kinetic viewpoint it seems that **Ru4(POM)** has several advantages, expressed in some order of magnitude, with respect to the IrO_2 nanoparticles, as far as Eq. (8) is concerned (and probably also for the successive Eqs. (9)–(11)). Obviously, the overall turnover frequency also depends on the rate constant of the process in Eq. (13) (the catalytic process), whose mechanism is however still not clarified. In any case, the fast hole scavenging processes involving **Ru4(POM)** would allow protection towards the stability of the overall photochemical water oxidation process, since the P^+ catalyst should be rapidly scavenged and therefore could not be affected (or affected only to a minor extent) by the decomposition reaction due to the oxygen produced.

Former studies have shown that the dendrimer species **4** has superior properties to $[Ru(bpy)_3]^{2+}$ as far as absorption of sunlight is concerned [63] and that **Ru4(POM)** has superior properties to

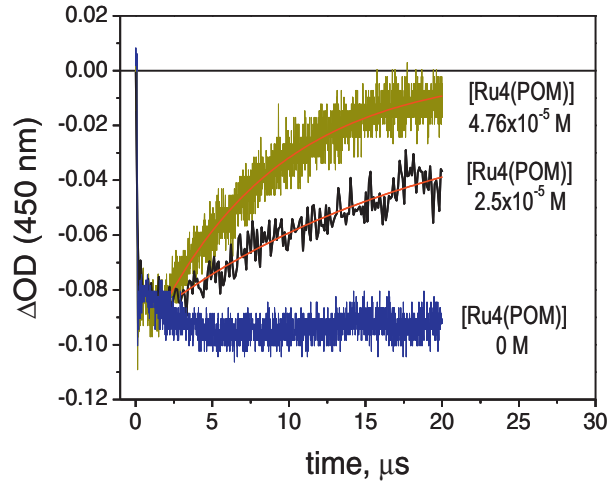

Fig. 9. Effect of added **Ru4(POM)** catalyst on the kinetics of disappearance of $[Ru(bpy)_3]^{3+}$, obtained by photooxidation of $[Ru(bpy)_3]^{2+}$ with persulfate. For experimental details, see Ref. [70].

IrO_2 nanoparticles from a kinetic viewpoint [70], the next step, then, was coupling **4** with **Ru4(POM)**. This was effectively made and quite interesting results were obtained [64]. Fig. 10 shows the time-profile of oxygen evolution during continuous irradiation of the a phosphate-buffered solution (pH = 7.2) containing **4**, **Ru4(POM)**, and persulfate: linear kinetics are maintained up to ca. 80% reaction within the overall experimental time (180 min). In this time frame, a O_2 evolution accounts for a persulfate conversion >90% (average yield over three runs). Similar results are obtained by using different buffers and pH conditions (Na_2SiF_6, 2.6×10^{-3} M/$Na_2B_4O_7$, 1.14×10^{-2} M; pH = 5.8). A direct comparison with a system in which malonate-stabilized IrO_2 nanoparticles are used as OEC instead of **Ru4(POM)** is shown in the same figure.

Beside the outstanding stability of the system (about 5% of photosensitizer degradation within the overall experimental time takes place), the most intriguing result obtained by this experiment is probably the photoreaction quantum yield. Indeed, a quite impressive quantum yield for oxygen production of 0.3 was calculated by irradiating at 550 nm [64]. This value, to the best of our knowledge, is the highest photoreaction quantum yield ever reported for photoinduced water oxidation, furthermore it was

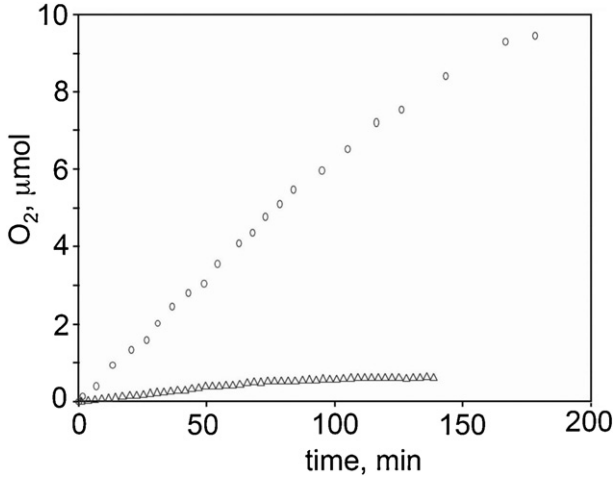

Fig. 10. Time profile of oxygen evolution during continuous irradiation (λ = 550 nm) of a phosphate-buffered solution of **4**, **Ru4(POM)**, and persulfate (circles). Diamonds shown the results obtained by using malonate-stabilized IrO_2 nanoparticles instead of **Ru4(POM)** in the same experimental conditions. For details, see Ref. [64].

obtained by using relatively long-wavelength light. Because of the absorption spectrum of **4**, it is foreseen that even light energy with λ over 700 nm can be used, without loss in quantum yield. Because the theoretical upper limit of photoreaction quantum yield in the present case is 0.5 (as already mentioned, the products of the reduction of the persulfate anion used as sacrificial agent oxidize a further molecule of sensitizer or catalyst by themselves for any photons processed by **4**, so that two photons are required to produce one O_2 molecule), about 60% of absorbed photons is used to produce oxygen. Possible reasons for such a result could include the expected advantage of using **4** instead of $[Ru(bpy)_3]^{2+}$-type compounds as far as the hole-scavenging reactions in Eqs. (8)–(11) are concerned, as already mentioned. In fact, the potential of the $\mathbf{4}^{+}$/**4** redox couple is +1.45 V whereas the that of $[Ru(bpy)_3]^{3+}$/$[Ru(bpy)_3]^{2+}$ is about 200 mV less favorable for the hole scavenging process. Moreover, it should not be neglected that possible ion pairing between the positively charged Ru-polypyridine sensitizers and the negatively charged **Ru4(POM)** catalyst could occur, so definitely favoring the rate constant of hole scavenging processes. Work is in progress in our laboratories to investigate this latter point.

6. Concluding remarks

The perfect machinery of Natural Photosynthesis, optimized through millennia of evolution, provides a highly efficient way to store and convert the solar radiation into chemical energy. This is a highly organized modular system with a unique ensemble of functional subtleties, powered by visible light and enabling a cascade of multi-electron/proton transfer and catalytic events with concerted rates. The artificial way can build on the natural hints, mimicking the photosynthetic assembly in vitro, and eventually surpassing evolution by devising new molecules and materials with enhanced stability and efficiency. Recent breakthroughs in this direction include: (i) the design of highly robust catalytic routines, enabling water oxidation with multi-turnover efficiency and remarkable speed and (ii) the tailored synthesis of antenna-like sensitizers, capable of photoinduced electron transfer under visible light irradiation. The next frontier is the rational organization of such functional units within a nanostructured environment, to promote any single event of the light/dark phases, while setting the required spatial proximity/geometry and avoid recombination/deactivation pathways finally relieving the fatigue of the catalytic routines. Such bottom-up approach to photosynthetic molecular materials will leverage some key improvements for the design of active systems finalized to the fabrication of innovative water splitting photoelectrodes and devices for a viable solar-driven hydrogen economy.

Acknowledgements

We thank the PRIN 20085ZXFEE for financial support.

References

[1] A.J. Bard, M.A. Fox, Acc. Chem. Res. 28 (1995) 141.
[2] N.S. Lewis, D.G. Nocera, Proc. Natl. Acad. Sci. U.S.A. 103 (2006) 15729.
[3] N. Armaroli, V. Balzani, Angew. Chem. Int. Ed. 46 (2007) 52.
[4] H.B. Gray, Nat. Chem. 1 (2009) 7.
[5] D. Gust, T.A. Moore, A.L. Moore, Acc. Chem. Res. 42 (2009) 1890.
[6] D.G. Nocera, D. Guldi (Guest Editors), Chem. Soc. Rev. 38 (2009) 1–293 (Special issue on Renewable Energy).
[7] L. Hammarström (Guest Editor), Acc. Chem. Res. 42 (2009) 1859–2029 (Special issue on Artificial Photosynthesis and Solar Fuels).
[8] M.H.V. Huynh, D.M. Dattelbaum, T.J. Meyer, Coord. Chem. Rev. 249 (2005) 457.
[9] V. Balzani, A. Credi, M. Venturi, ChemSusChem 1 (2008) 26.
[10] M. Wasielewski, Acc. Chem. Res. 42 (2009) 1910.
[11] (a) B. Albinsson, J. Mårtensson, J. Photochem. Photobiol. C 9 (2008) 138; (b) A. Magnuson, M. Anderlund, O. Johansson, P. Lindblad, R. Lomoth, T. Polivka, S. Ott, K. Stensjö, S. Styring, V. Sundström, L. Hammarström, Acc. Chem. Res. 42 (2009) 1899.

[12] (a) D. Gust, T.A. Moore, A.L. Moore, Acc. Chem. Res. 34 (2001) 40;
(b) M. Hambourger, G. Kodis, M.D. Vaughn, G.F. Moore, D. Gust, A.L. Moore, T.A. Moore, Dalton Trans. (2009) 9979.
[13] A.C. Benniston, A. Harriman, Mater. Today 11 (2008) 376.
[14] J.P. McEvoy, G.W. Brudvig, Chem. Rev. 106 (2006) 4455.
[15] (a) M.H.V. Huynh, T.J. Meyer, Chem. Rev. 107 (2007) 5004;
(b) T.J. Meyer, M.H.V. Huynh, H.H. Thorp, Angew. Chem. Int. Ed. 48 (2007) 5284.
[16] F. Liu, J.J. Concepcion, J.W. Jurss, T. Cardolaccia, J.L. Templeton, T.J. Meyer, Inorg. Chem. 47 (2008) 1697.
[17] T.J. Meyer, Nature 451 (2008) 778.
[18] K.N. Ferreira, T.M. Iverson, K. Maghlaoui, J. Barber, S. Iwata, Science 303 (2004) 1831.
[19] B. Kok, B. Forbush, M. McGloin, Photochem. Photobiol. 11 (1970) 457.
[20] H. Dau, M. Haumann, Coord. Chem. Rev. 252 (2008) 273.
[21] S.W. Gersten, G.J. Samuels, T.J. Meyer, J. Am. Chem. Soc. 104 (1982) 4029.
[22] (a) F. Liu, J.J. Conception, J.W. Jurss, T. Cardolaccia, J.L. Templeton, T.J. Meyer, Inorg. Chem. 47 (2008) 1727;
(b) J.W. Jurss, J.C. Concepcion, M.R. Norris, J.L. Templeton, T.J. Meyer, Inorg. Chem. 49 (2010) 3980.
[23] Z. Deng, H.-W. Tseng, R. Zong, D. Wang, R.P. Thummel, Inorg. Chem. 47 (2008) 1835.
[24] (a) T. Wada, K. Tsuge, K. Tanaka, Inorg. Chem. 40 (2001) 329;
(b) L. Duan, Y. Xu, P. Zhang, M. Wang, L. Sun, Inorg. Chem. 49 (2010) 209;
(c) Y. Xu, L. Duan, L. Tong, B. Akermark, L. Sun, Chem. Commun. 46 (2010) 6506;
(d) F. Borzoglian, J. Mola, M. Rodriguez, I. Romero, J. Nenet-Buchholtz, X. Fontrodona, C.J. Cramer, L. Gagliardi, A. Llobet, J. Am. Chem. Soc. 131 (2009) 15176.
[25] A. Sartorel, M. Carraro, G. Scorrano, R. De Zorzi, S. Geremia, N.D. McDaniel, S. Bernhard, M. Bonchio, J. Am. Chem. Soc. 130 (2008) 5006.
[26] Y.V. Geletii, B. Botar, P. Köegerler, D.A. Hillesheim, D.G. Musaev, C.L. Hill, Angew. Chem. Int. Ed. 47 (2008) 3896.
[27] N.D. McDaniel, M.J. Coughlin, L.L. Tinker, S. Bernhard, J. Am. Chem. Soc. 130 (2008) 210.
[28] (a) J. Limburg, J.S. Vrettos, L.M. Liable-Sands, A.L. Rheingold, R.H. Crabtree, G.W. Brudvig, Science 283 (1999) 1524;
(b) C.W. Cady, R.H. Crabtree, G.W. Brudvig, Coord. Chem. Rev. 252 (2008) 444;
(c) R. Tagore, R.H. Crabtree, G.W. Brudvig, Inorg. Chem. 47 (2008) 1815.
[29] (a) G.C. Dismukes, R. Brimblecomb, G.A. Felton, R.S. Pryadun, J.E. Sheats, L. Spiccia, G.F. Swiegers, Acc. Chem. Res. 42 (2009) 1935;
(b) D.M. Robinson, Y.B. Go, M. Greenblatt, C.G. Dismukes, J. Am. Chem. Soc. 132 (2010) 11467.
[30] Q. Yin, J.M. Tan, C. Besson, Y.V. Geletii, D.G. Musaev, A.E. Kuznetsov, Z. Luo, K.I. Hardcastle, C.L. Hill, Science 328 (2010) 342.
[31] W.C. Ellis, N.D. McDaniel, S. Bernhard, T.J. Collins, J. Am. Chem. Soc. 132 (2010) 10990.
[32] J.J. Concepcion, J.W. Jurss, J.L. Templeton, T.J. Meyer, J. Am. Chem. Soc. 130 (2008) 16462.
[33] R. Zong, R.P. Thummel, J. Am. Chem. Soc. 127 (2005) 12802.
[34] H. Kunkely, A. Vogler, Angew. Chem. Int. Ed. 48 (2009) 1685.
[35] (a) F. Jiao, H. Frei, Angew. Chem. Int. Ed. 48 (2009) 1841;
(b) F. Jiao, H. Frei, Energy Environ. Sci. 3 (2010) 1018.
[36] Y. Gorlin, T.F. Jamarillo, J. Am. Chem. Soc. 132 (2010) 13612.
[37] A. Harriman, M. Richoux, P.A. Christensen, S. Moseri, P. Neta, J. Chem. Soc. Faraday Trans. I 83 (1987) 3001, and refs. therein.
[38] N.D Morris, M. Suzuki, T.E. Mallouk, J. Phys. Chem. A 108 (2004) 9115.
[39] M. Hara, C.C. Waraksa, J.T. Lean, B.A. Lewis, T.E. Mallouk, J. Phys. Chem. A 104 (2000) 5275.
[40] P.G. Hoertz, Y.-I. Kim, W.J. Youngblood, T.E. Mallouk, J. Phys. Chem. B 111 (2007) 6845.
[41] M.W. Kanan, D.G. Nocera, Science 321 (2008) 1072.
[42] T.A. Betley, Q. Wu, T. Van Voorhis, D.G. Nocera, Inorg. Chem. 47 (2008) 1849.
[43] Y. Surendranath, M. Dinca, D.G. Nocera, J. Am. Chem. Soc. 131 (2009) 2615.
[44] D.A. Lutterman, Y. Surendranath, D.G. Nocera, J. Am. Chem. Soc. 131 (2009) 3839.
[45] (a) S.W. Kohl, L. Weiner, L. Schwartsburd, L. Konstantinovski, L.J.W. Shimon, Y. Ben-David, M.A. Iron, D. Milstein, Science 324 (2009) 74;
(b) H.J.M. Hou, J. Integr. Plant Biol. 52 (2010) 704, and refs. therein.
[46] (a) H. Yamazaki, A. Shouji, M. Kajita, M. Yagi, Coord. Chem. Rev. 254 (2010) 2483;
(b) M. Yagi, M. Toda, S. Yamada, H. Yamazaki, Chem. Commun. (2010), doi:10.1039/c0cc03114c.
[47] J.L. Cape, J.K. Hurst, J. Am. Chem. Soc. 130 (2008) 827.
[48] D.K. Zhong, D.R. Gamelin, J. Am. Chem. Soc. 132 (2010) 4202.
[49] R. Brimblecomb, A. Koo, G.C. Dismukes, G.F. Swiegers, L. Spiccia, J. Am. Chem. Soc. 132 (2010) 2892.
[50] (a) L. Li, L. Duan, Y. Xu, M. Gorlov, A. Hagfeldt, L. Sun, Chem. Commun. 46 (2010) 7307;
(b) Y. Xu, A. Fischer, L. Duan, L. Tong, E. Gabrielsson, B. Akermark, L. Sun, Angew. Chem. Int. Ed. (2010), doi:10.1002/anie.201004278.
[51] Y.S. Nam, A.P. Magyar, D. Lee, J.-W. Kim, D.S. Yun, H. Park, T.S. Pollom, D.A. Weitz, A.M. Belcher, Nat. Nanotechnol. 5 (2010) 340.
[52] A. Juris, V. Balzani, F. Barigelletti, S. Campagna, P. Belser, A. von Zelewsky, Coord. Chem. Rev. 84 (1988) 85.
[53] T.J. Meyer, Pure Appl. Chem. 58 (1986) 1193.
[54] S. Campagna, G. Denti, S. Serroni, A. Juris, M. Venturi, V. Ricevuto, V. Balzani, Chem. Eur. J. 1 (1995) 211.
[55] S. Serroni, A. Juris, M. Venturi, S. Campagna, I. Resino Resino, G. Denti, A. Credi, V. Balzani, J. Mater. Chem. 7 (1997) 1227.
[56] V. Balzani, S. Campagna, G. Denti, A. Juris, S. Serroni, M. Venturi, Acc. Chem. Res. 31 (1998) 26.
[57] M. Venturi, S. Serroni, A. Juris, S. Campagna, V. Balzani, Top. Curr. Chem. 197 (1998) 193.
[58] S. Serroni, S. Campagna, F. Puntoriero, C. Di Pietro, F. Loiseau, N.D. McClenaghan, Chem. Soc. Rev. 30 (2001) 367.
[59] F. Puntoriero, S. Serroni, M. Galletta, A. Juris, A. Licciardello, C. Chiorboli, S. Campagna, F. Scandola, ChemPhysChem 6 (2005) 129.
[60] J. Larsen, F. Puntoriero, T. Pascher, N. McClenaghan, S. Campagna, E. Åkesson, V. Sundström, ChemPhysChem 8 (2007) 2643.
[61] W.J. Youngblood, S.-H.A. Lee, Y. Kobayashi, E.A. Hernandez-Pagan, P.G. Hoertz, T.A. Moore, A.L. Moore, D. Gust, T.E. Mallouk, J. Am. Chem. Soc. 131 (2009) 926.
[62] (a) K. Kalyanasundaram, Photochemistry of Polypyridine and Porphyrin Complexes, Academic, New York, 1992;
(b) V. Balzani, F. Scandola, Supramolecular Photochemistry, Horwood, Chichester, 1991.
[63] G. La Ganga, F. Nastasi, S. Campagna, F. Puntoriero, Dalton Trans. (2009) 9997.
[64] F. Puntoriero, G. La Ganga, A. Sartorel, M. Carraro, G. Scorrano, M. Bonchio, S. Campagna, Chem. Commun. 46 (2010) 4725.
[65] J.W. Youngblood, S.-H.A. Lee, K. Maeda, T.E. Mallouk, Acc. Chem. Res. 42 (2009) 1966.
[66] A. Sartorel, P. Mirò, E. Salvadori, S. Romain, M. Carraro, G. Scorrano, M. Di Valentin, A. Llobet, C. Bo, M. Bonchio, J. Am. Chem. Soc. 131 (2009) 16051.
[67] F.M. Toma, A. Sartorel, M. Iurlo, M. Carraro, P. Parisse, C. Maccato, S. Rapino, B. Rodriguez Gonzales, H. Amenitsch, T. De Ros, L. Casalis, A. Goldoni, M. Marcaccio, G. Scorrano, G. Scoles, F. Paolucci, M. Prato, M. Bonchio, Nat. Chem. 2 (2010) 826.
[68] Y.V. Geletii, Z. Huang, Y. Hou, D.G. Musaev, T. Lian, C.L. Craig, J. Am. Chem. Soc. 131 (2009) 7522.
[69] X. Sala, I. Romero, M. Rodriguez, L. Escriche, A. Llobet, Angew. Chem. Int. Ed. 48 (2009) 2842.
[70] M. Orlandi, R. Argazzi, A. Sartorel, M. Carraro, G. Scorrano, M. Bonchio, F. Scandola, Chem. Commun. 46 (2010) 3152.